X-Ray CT Scatter Correction by a Physics Motivated DNN with Opposite View Processing

Berk Iskender and *Yoram Bresler*

Coordinated Science Lab and Department of ECE
University of Illinois, Urbana-Champaign

The 6th International Conference on Image Formation in X-Ray Computed Tomography

ECE ILLINOIS

This work was supported in part by the National Science Foundation (NSF) under Grant IIS 14-47879.

Problem Statement

Assumption: Beer's Law

$$\boxed{p(t,\theta) = I_0 e^{-g(t,\theta)},\ \ g(t,\theta) = (Rf)(t,\theta)}$$

I_0: *vacuum (air) measurement*, $f(\boldsymbol{x})$: *object*, $x \in \mathbb{R}^2$, R: *2D Radon transform*
p: *primary measurement*, g: *line integral projection*, $t \in \mathbb{R}^d$, $\theta \in [0, 2\pi)$

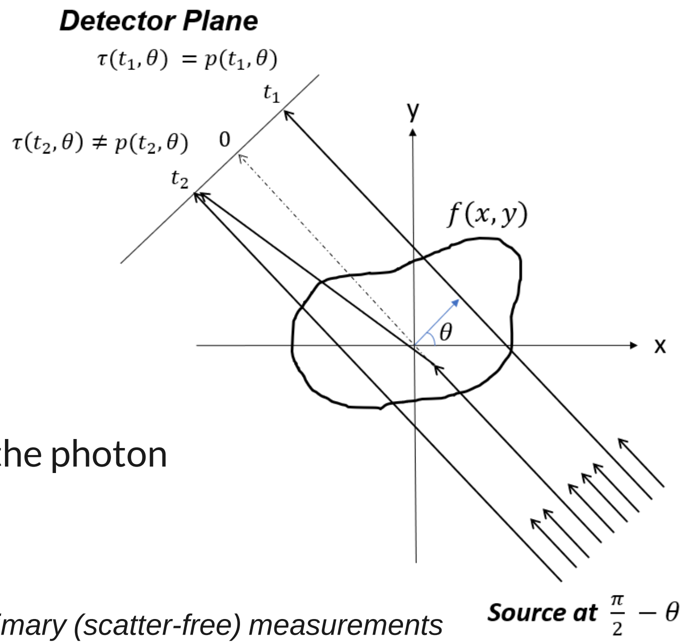

- **Reality:** Scattering causes a <u>change in the direction</u> (and energy) of the photon

$$\tau(t,\theta) = p(t,\theta) + s(t,\theta), \qquad s(t,\theta) \geq 0$$

$\tau \triangleq \{\tau_\theta, \theta \in \Theta\}$: *Set of total (scatter corrupted) measurements*, $p \triangleq \{p_\theta, \theta \in \Theta\}$: *Set of primary (scatter-free) measurements*

$s \triangleq \{s_\theta, \theta \in \Theta\}$: *Scatter term* ***(nonlinear function of f)***

Reconstruction

I_0: *vacuum (air) measurement*,

R^{-1}: *FBP algorithm*

$$\text{Scatter} - \text{free:}\ \ g(t,\theta) = -\ln\frac{p(t,\theta)}{I_0} \ \rightarrow\ f(\boldsymbol{x}) = (R^{-1}g)(\boldsymbol{x})$$

$$g(t,\theta) = -\ln\frac{\tau(t,\theta)}{I_0} = -\ln\frac{p(t,\theta)+s(t,\theta)}{I_0} \ \Rightarrow\ \tilde{f}(x) = \left(R^{-1}\tilde{g}\right)(x) \neq f(x)$$

Proposed Method

- A new physics-motivated, deep learning-based method to estimate and correct scatter in projection measurements

- New features: **1)** Incorporates both **scatter-corrupted measurements** τ_θ + **initial reconstruction** $\tilde{f}_\theta$

  ⟹ Scatter estimate for each view angle θ depends on the entire object

  2) Uses **equality** (up to flip) of scatter-free **projections in opposite directions**

  3) DCNN **architecture** inspired by scatter-physics

  4) For training, uses a **physics-adapted loss function**

- Operates on normalized quantities, $\bar{\tau}_\theta = \tau_\theta / I_0$, $\bar{p}_\theta = p_\theta / I_0$, $\bar{s}_\theta = s_\theta / I_0$ ⟶ applicable for various I_0

Opposite View Processing

- π-*opposite* view projections are identical (up to a flip in t) $\Rightarrow$ $\hat{g}(t,\theta+\pi) \triangleq g(-t,\theta+\pi) = g(t,\theta)$
- Difference of π-*opposite* scatter components: $\tau_\theta - \hat{\tau}_{\theta+\pi} = \cancel{p_\theta} + s_\theta - \cancel{\hat{p}_{\theta+\pi}} - \hat{s}_{\theta+\pi} \triangleq \Delta s_\theta$
- Needs to be estimated: $b_\theta \triangleq s_\theta + \hat{s}_{\theta+\pi}$

- Δs_θ higher bandwidth & b_θ typically smoother $\Rightarrow$ b_θ may be easier to estimate by a DCNN

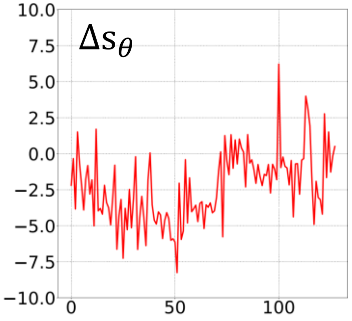

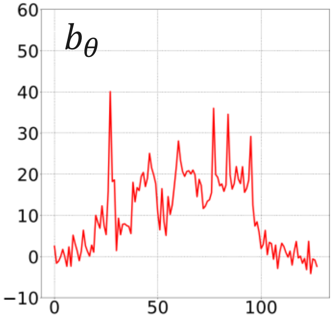

- Finally, $p_\theta = \dfrac{\tau_\theta + \hat{\tau}_{\theta+\pi} - b_\theta}{2}$

Block Diagram & Loss Function

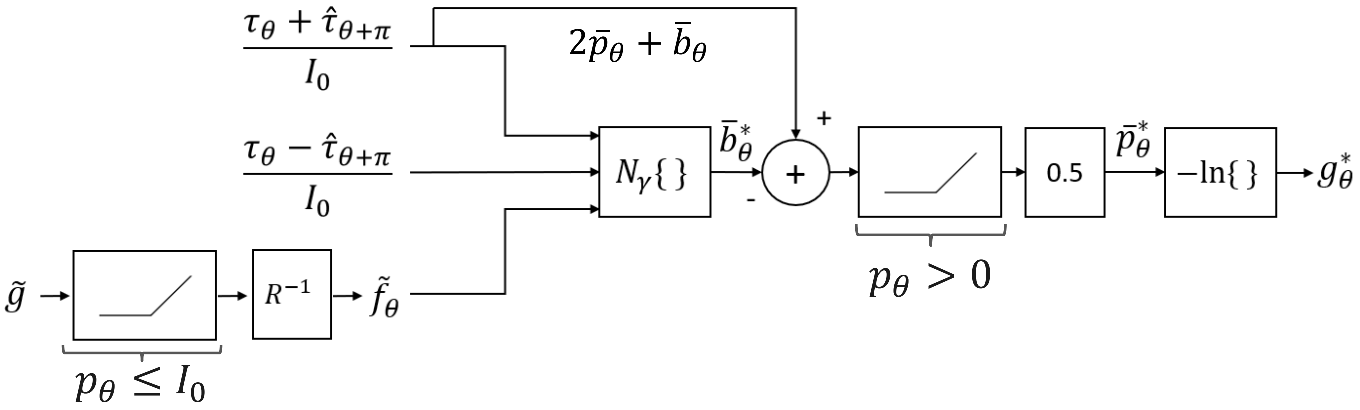

- After processing all views,

$$f^*(\boldsymbol{x}) = (R^{-1}g^*)(\boldsymbol{x})$$

Loss function, L, for training the network:

$$L(g, g^*) = \min_{\gamma} \sum_{\theta \in \Theta} \|h * (g_\theta - g^*_\theta)\|_2^2 + \lambda \|g_\theta - g^*_\theta\|_1$$

- $h[n] = \frac{1}{2}\delta[n+1] - \frac{1}{2}\delta[n-1]$, $\lambda > 0$
- **L is tailored to express errors in the reconstructed image,** $f^*(\boldsymbol{x})$

(1) Particular h selection

(2) Post-log quantities g are used rather than p

Filter h

- Enables to express the norm of **an image-domain error** in **the projection domain** ⟶ **No need for FBP in L**

  ($||Qf||_2$ in terms of g_θ, Q: a radially symmetric filter)

- Edges are perceptually significant ⟶ Q is HPF

- Using Parseval's identity & projection-slice theorem ⟶ $\boxed{\|Qf\|_2^2 = \|h * g\|_2^2}$

- Using Shepp-Logan filter in FBP and $Q(\nu) = |\nu|^{0.5}$ ⟶ *Short time-domain filter*

$$\boxed{h[n] = \frac{1}{2}\delta[n+1] - \frac{1}{2}\delta[n-1]}$$

DCNN, N_γ

- Inspired by the Slice-by-Slice approach (Bai *et al* 2000)
- Inputs:
    i. Sum of pre-log π-opposite total measurements at θ: $\bar{\tau}_\theta + \hat{\bar{\tau}}_{\theta+\pi} \in \mathbb{R}^d$
    ii. Difference of same measurements at θ: $\bar{\tau}_\theta - \hat{\bar{\tau}}_{\theta+\pi} \in \mathbb{R}^d$
    iii. Initial reconstruction estimate, rotated by θ: $\tilde{f}_\theta \in \mathbb{R}^{d^2}$
- Output:
    i. Normalized scatter component estimate: $\bar{s}_\theta^* = N_\gamma\left(\tilde{f}_\theta, \bar{\tau}_\theta + \hat{\bar{\tau}}_{\theta+\pi}, \bar{\tau}_\theta - \hat{\bar{\tau}}_{\theta+\pi}\right) \in \mathbb{R}^d$

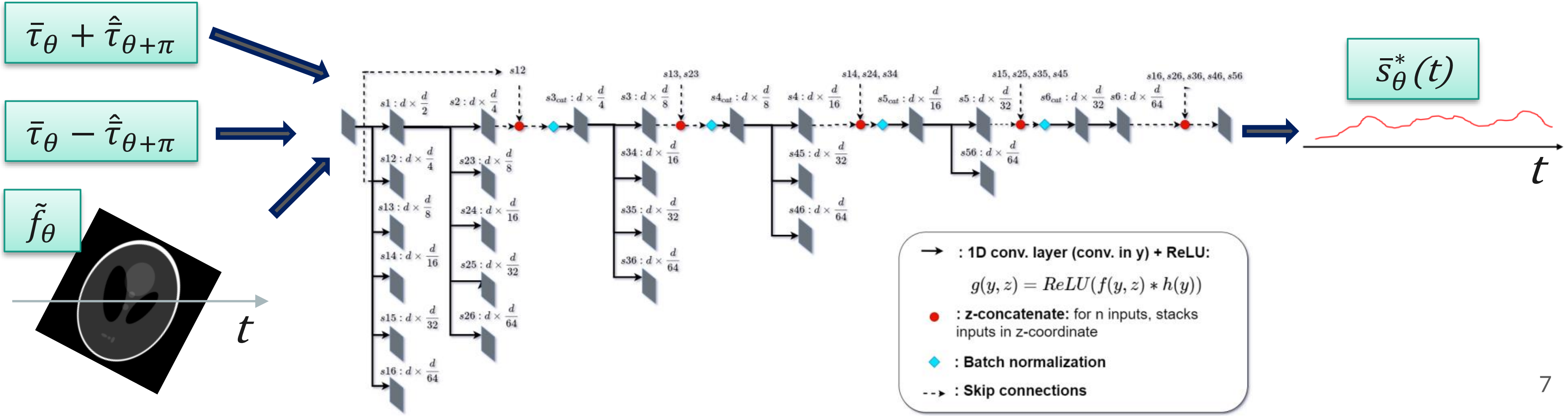

Results

Ground Truth f

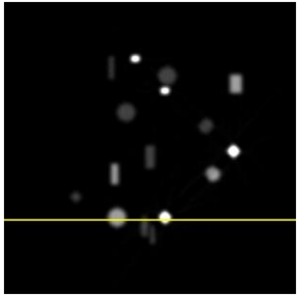

using primary meas. p_θ

	Uncor.	DSE-1D	Proposed SW	Proposed
PSNR	31.05	37.19	43.83	**45.90**
SSIM	0.92	0.90	**0.98**	**0.98**
MAE	42.4	38.3	**14.5**	15.3

Table: Average reconstruction accuracies

Recovered f^*

Recon Error: $\Delta f = f - \tilde{f}$

1D line profiles

Uncorrected

DSE-1D†

Proposed – Single View

Proposed

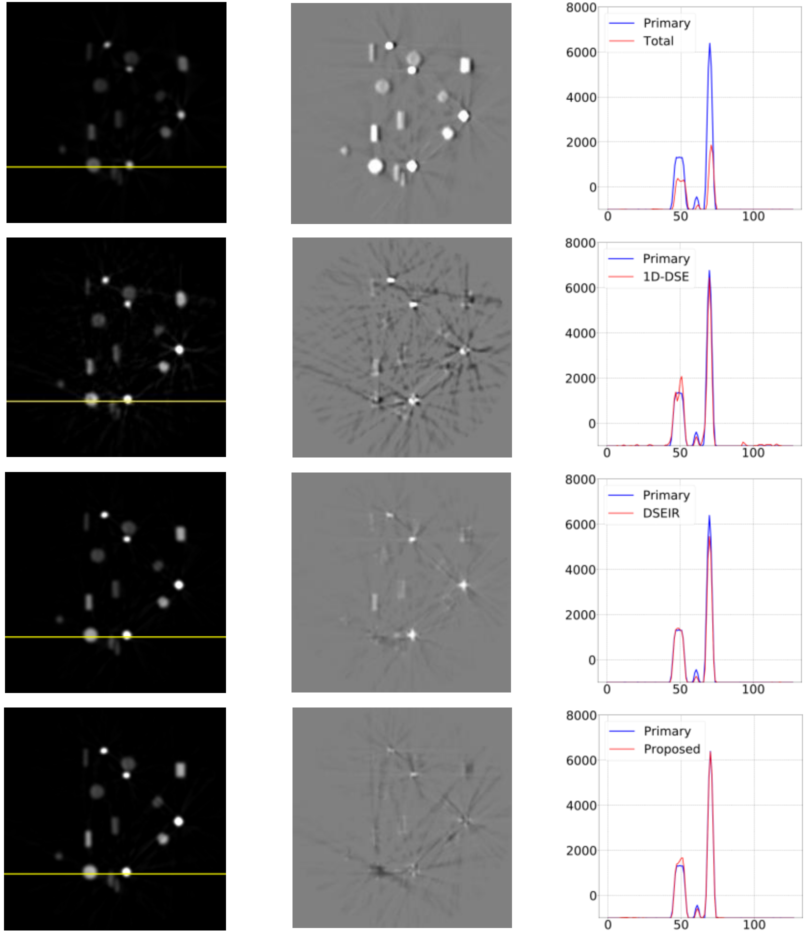

† J. Maier et al., “Deep Scatter Estimation (DSE): Accurate real-time scatter estimation for X-ray CT using a deep convolutional neural network,” *Jour. of Nondest. Eval.*, vol. 37, no. 3, 2018.

Conclusions

- Scattering in X-ray CT produces various degradations in the reconstructions
- A data-driven approach with using both scatter-corrupted meas. and initial reconstruction

  DCNN architecture inspired by scatter-physics

  physics-motivated cost function and constraints

  leveraging $\pi - opposite$ equality of projections
- Performs better compared to other methods

Future Work

- Implementing the method for other CT geometries
- Extending the experiments to polychromatic beam setting & 3D reconstructions

References

1. Floyd C E, Jaszczak R J, Harris C C and Coleman R E 1984 Energy and spatial distribution of multiple order Compton scatter in SPECT: a Monte Carlo investigation *Phys. Med. Biol.* **29** 1217-30
2. H. E. Johns and J. R. Cunningham, *The physics of Radiology*, *Third edition* (Thomas, Springfield, Illinois, 1971), p. 167.
3. Poludniowski, G., et al. "An efficient Monte Carlo-based algorithm for scatter correction in keV cone-beam CT." *Physics in Medicine & Biology* 54.12 (2009): 3847.
4. C. Bai, G. L. Zeng, and G. T. Gullberg, "A slice-by-slice blurring model and kernel evaluation using the Klein Nishina formula for 3D scatter compensation in parallel and converging beam spect," *Phys. Med. Biol.*, vol. 45, no. 5, 2000.
5. B. Iskender and Y. Bresler, "A Physics-Motivated DNN for X-Ray CT Scatter Correction," *2020 IEEE 17th International Symposium on Biomedical Imaging (ISBI)*, Iowa City, IA, USA, 2020.
6. A. Maslowski et al., "Acuros CTS: A fast, linear Boltzmann transport equation solver for computed tomography scatter–Part I: Core algorithms and validation", *Med. Phys.*, vol. 45, no. 5, 2018
7. B Ohnesorge, T Flohr, and K Klingenbeck-Regn, "Efficient object scatter correction algorithm for third and fourth generation CT scanners," *European radiology*, vol. 9, no. 3, 1999.
8. J. Maier et al., "Deep Scatter Estimation (DSE): Accurate real-time scatter estimation for X-ray CT using a deep convolutional neural network," *Jour. of Nondest. Eval.*, vol. 37, no. 3, 2018.